Ultrawide tuning of photonic microcavities via evanescent field perturbation

Peter T. Rakich, Miloš A. Popović, Michael R. Watts, Tymon Barwicz, Henry I. Smith, and Erich P. Ippen

Research Laboratory of Electronics, Massachusetts Institute of Technology, 77 Massachusetts Avenue, Cambridge, Massachusetts 02139

Received December 15, 2005; accepted January 4, 2006; posted January 31, 2006 (Doc. ID 66438)

Evanescent field perturbation of an integrated microring resonator is examined as a means of achieving high-fidelity reversible tuning of photonic microcavities over large wavelength ranges. A 1.7% wavelength tuning is achieved through the use of a novel silica fiber probe that provides access to the evanescent field of an air-clad high-index-contrast ring resonator. As the microring is perturbed, the probe–ring distance is found through simultaneous nanometric distance calibration and force measurements. Experimental results agree well with theoretical tuning. Possible microelectromechanical systems implementation of this effect is discussed, as well as avenues for improvement of the tuning range. © 2006 Optical Society of America

OCIS codes: 130.3120, 230.5750, 230.7370.

The field of integrated optics promises to provide a practical and scalable means of routing and switching light for applications ranging from telecommunications networks to sensing and spectroscopy. However, a practical means of creating large changes in waveguide effective index (Δn_{eff}) does not exist in microphotonics, forming a key barrier to the development of dynamic integrated optical circuits. A large Δn_{eff} is critical for the development of widely tunable filters and for scaling active components to smaller size. Currently, thermo-optical tuning is the only widely implemented means of producing Δn_{eff} in integrated circuits,[1–3] but it has insufficient range and is slower than desired for many applications.

In this Letter we demonstrate ultrawide tunability through evanescent perturbation of a large free-spectral-range microring resonator. Geometrical tuning mechanisms, such as evanescent tuning, have the distinct advantages that they are material-system independent, and they make possible large Δn_{eff} with small power dissipation. In what follows, a 1.7% wavelength shift (or 27 nm tuning at 1565 nm) is demonstrated in a microring resonator without resolvable distortion of the cavity resonance. Furthermore, complete recovery of the resonance is found when the perturbing body is removed. Experiments are carried out with a novel silica fiber probe that provides access to the evanescent field of an air-clad high-index-contrast ring resonator mode. As the probe is advanced toward the ring resonator, the probe–ring distance is found through simultaneous nanometric distance calibration and force measurements.

For this study, a silicon nitride ring resonator of the type described in Ref. 4, but of first order, is considered. The ring resonator was designed for operation near 1.5 μm wavelengths and has a free spectral range of 27 nm. The transmitted (through) and resonantly dropped (drop) powers are shown as functions of wavelength in Fig. 1(a). The mode of the air-clad ring resonator has an evanescent field extending outside the guide in the direction normal to the plane of the ring. Consequently, a dielectric body can be placed above the ring such that it uniformly penetrates the evanescent field of the ring [see the inset of Fig. 1(b)]. This produces an increase in the effective index of the mode, resulting in a shift of resonance frequency.

Perturbation of the ring is considered with a uniform silica slab ($n=1.45$). The change in resonance wavelength ($\Delta\lambda$) as a function of the slab–ring separation (z) can be approximated from the effective index (n_{eff}) and the group index (n_{group}) of the perturbed waveguide mode. The resonance condition of the ring mode is $kn_{\text{eff}}L=2\pi m$, where k, L, and m are the free-space wavenumber, the path length of the ring, and an integer resonance index, respectively. Through perturbative expansion of this relation with respect to λ and n_{eff} one finds a shift in resonance wavelength given by

$$\Delta\lambda/\lambda \approx \Delta n_{\text{eff}}/n_{\text{group}}. \quad (1)$$

Here, Δn_{eff} is the change in effective index induced by the perturbing slab. Equation (1) is used in conjunction with a full-vectorial mode solver to compute wavelength shift induced by a silica slab. The results of the perturbative computation are plotted in Fig. 1(b), displaying a maximum theoretical tuning range of 28.5 nm at an operating wavelength of 1565 nm. The computed wavelength shift closely approximates an exponential, with a decay length of 89.3 nm, making it evident that a high degree of positional control is required.

The major challenge in laboratory implementation of the geometry shown in Fig. 1(b) is the high degree of angular alignment required between the perturbing body and the ring resonator (typically $\sim$100 μrad). This alignment issue is addressed through the novel probe design illustrated in Fig. 2(a). The design utilizes a fiber taper near the end of the probe, which allows the fiber end to lie parallel to the surface when it comes in contact with the substrate of the ring resonator. The fabrication process for this probe is outlined in the inset of Fig. 2(a). First, the fiber (125 μm diameter) is tapered to several micrometers, forming a flexible joint. Then the

0146-9592/06/091241-3/$15.00

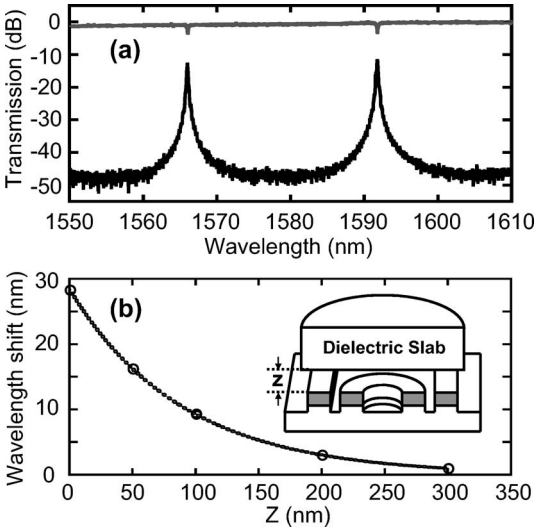

Fig. 1. (a) Through (upper) and drop (lower) responses of the fabricated microring. (b) Computed tuning versus height, z, of the perturbing body above the microring (circles), exponential fit (dashed curve). Schematic of tuning geometry (inset).

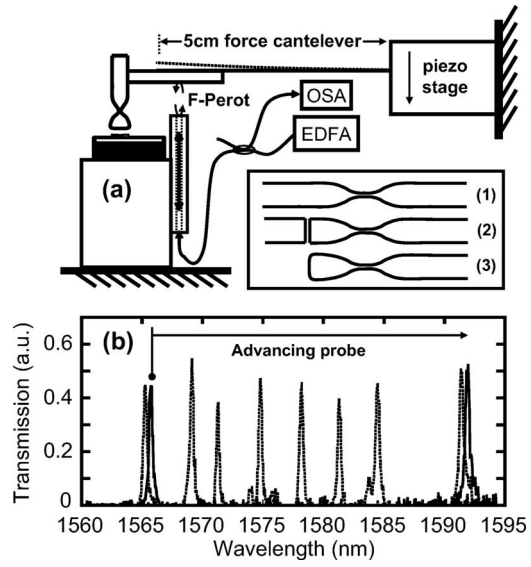

Fig. 2. (a) Diagram of tuning apparatus and fiber-probe fabrication process (inset), (b) Characteristic drop spectra as the probe is advanced toward the microring. Unperturbed (solid curve) and increasing microring perturbation (dashed curve).

face of the probe (used to perturb the ring resonator) is formed by a fiber cleave and annealed until a small amount of glass reflow occurs, ensuring an ultrasmooth surface.

The apparatus used to perform evanescent perturbation experiments can be seen in Fig. 2(a). It consists of the silica fiber probe (described above), which is mounted on a 5 cm cantilever with a force constant of ~5000 N/m. The probe–cantilever assembly is mounted on a distance-calibrated piezo translation stage such that it can be brought in and out of contact with the ring resonator device. The motion of the cantilever and the probe relative to the device is monitored with a Fabry–Perot (F-Perot) interferometer, one end of which is formed by the cantilever. The position of the probe is read through rapid interrogation of the interferometer with white light from an erbium-doped fiber amplifier (EDFA) and an optical spectrum analyzer (OSA). The force experienced by the probe can be precisely measured from the cantilever deflection (obtained from the difference between the interferometer and stage displacements). Broadband EDFA light is also coupled into and collected from the ring resonator device with lensed fibers, permitting rapid spectral acquisitions (~100 μs snapshots) of the ring drop response with a monochromator and a InGaAs camera [see Fig. 2(b)]. Experiments were performed by simultaneously measuring the ring resonator drop response, cantilever position, and forces of probe–sample interaction.

The results of a tuning experiment can be seen in Figs. 3(a)–3(c). Figure 3(a) shows the ring resonance frequency as a function of the cantilever position measured by the interferometer. Each data point (circle) represents the resonant wavelength obtained from a drop port measurement of the microring. The force and force derivative experienced by the probe over the same range of cantilever displacement are displayed in Figs. 3(b) and 3(c). In Fig. 3(a) two trends can be seen: (1) for smaller positions (i.e., $\leqslant$1270 nm) an exponential change in resonance wavelength occurs over a 25 nm tuning, (2) for positions larger than 1270 nm (indicated by the vertical dashed line) there is a very gradual change in ring resonance frequency. In interpreting these two tuning regimes, the forces of interaction between the probe and sample [seen in Fig. 3(b)] provide insight. Over the exponential tuning regime, attractive forces (negative in sign) are experienced by the probe. These are likely a combination of capillary and van der Waals interactions as the probe approaches flush contact.[5] Snap-down of the probe can be seen at 1270 nm most clearly through a sharp decrease in

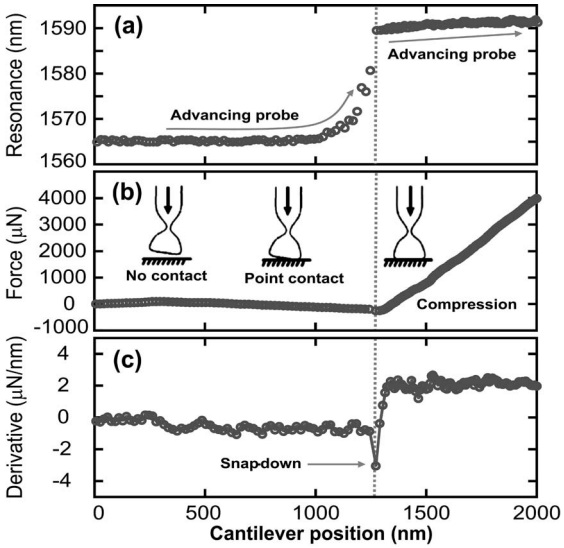

Fig. 3. (a) Measured resonance frequency of ring resonator (from drop response) versus cantilever displacement, (b) Force of probe–ring interaction and (c) force derivative versus position. The sharp discontinuity at 1270 nm indicates snap-down of the probe due to attractive forces.

the derivative of the force, corresponding to the maximum in the exponential portion of the tuning curve. After this point, the probe remains flush with the surface of the device, resulting in elastic compression of the probe, which is seen as a large positive slope in the force curve. Note that in all cases the forces applied are far smaller than those required to generate commensurate strain-based tuning, indicating that the gradual tuning observed after snap-down results from a small final change in probe conformation.

By use of the snap-down position found from the force and force derivative measurements, the probe–ring distance can be placed on an absolute scale and compared with theory, as seen in Fig. 4. An exponential fit of the tuning versus probe–ring distance reveals a decay length of 87±4 nm and a maximum tuning of 24.8 nm, which agrees with the theoretical decay length of 89.3 nm and maximum tuning range of 28.5 nm. Tuning ranges of 25–27 nm were also obtainable by bringing the ring in contact with various points of the probe face, indicating that slight asymmetries of the probe surface [generated through step (3) of fabrication] play a role in limiting the maximum perturbation possible. It is important to note that throughout the tuning process the resonance shape appears to be roughly preserved. A relatively constant drop efficiency can be seen in Fig. 2(b), indicating that the ring quality factor (Q) is not significantly altered [small variations in drop efficiency, seen in Fig. 2(b), are more likely a result of the poor signal-to-noise experienced when acquiring spectra at high speeds]. Additionally, when the fiber is raised again, the unperturbed resonance is fully recovered (Fig. 4, inset), demonstrating a negligible degree of hysteresis and suggesting no material exchange between the probe and ring.

In conclusion, high-fidelity reversible tuning was demonstrated over a 1.7% frequency range through evanescent-field perturbation of a microring. In this experiment, a uniform silica perturbing body was used, although it should be noted that with a higher-index perturbing structure upwards of 3% tuning could be implemented through the same range of motion. Furthermore, higher-index-contrast wave guides, such as silicon, can tolerate higher index perturbation before coupling to radiation modes occurs, making possible considerably larger timing ranges. Similar opportunities for evanescent tuning exist in a photonic crystal platform through a natural extension of the concept applied here.

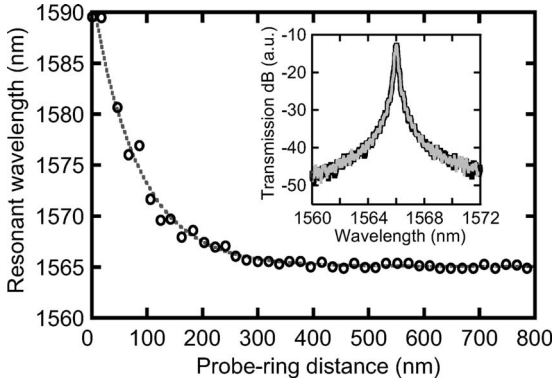

Fig. 4. Tuning versus distance from probe snap-down (circles) with exponential fit (dashed curve). Inset, drop measured before (black) and after (gray) a tuning experiment.

Ultimately microelectromechanical system (MEMS) implementation of this tuning mechanism through a device similar to that described in Ref. 6 would be ideal, as it would require negligible power dissipation and could permit rapid switching times (microseconds to nanoseconds). However, the attractive forces between the perturbing body and the ring surface must be mitigated to ensure that snap-down does not disrupt the device behavior. Additionally, due to the sensitivity of this tuning mechanism to the position of the perturbing body, careful consideration of thermally induced vibrations must be made in designing a MEMS device.[7–9]

We thank Hermann A. Haus for inspiration and guidance, and George Barbastathis, Greg Nielson, Marcus Dahlem, Daniel Sparacin, and Thomas Schibli for helpful technical discussions. We gratefully acknowledge financial support from Pirelli Labs S.p.A., Defence Advanced Research Projects Agency, Department of Defense (Office of Naval Research) Multi-University Research Initiative, and the U.S. Air Force Office of Scientific Research for financial support. P. T. Rakich's e-mail address is rakich@mit.edu.

References

1. P. Heimala, P. Katila, J. Aarnio, and A. Heinamaki, J. Low Temp. Phys. **14**, 2260 (1996).
2. D. Geuzebroek, E. Klein, H. Kelderman, N. Baker, and A. Driessen, IEEE Photon. Technol. Lett. **17**, 336 (2005).
3. H. M. H. Chong and R. M. De La Rue, IEEE Photon. Technol. Lett. **16**, 1528 (2004).
4. T. Barwicz, M. A. Popović, P. T. Rakich, M. R. Watts, H. A. Haus, E. P. Ippen, and H. I. Smith, Opt. Express **12**, 1437 (2004).
5. W. M. van Spengen, R. Puers, and I. De Wolf, J. Micromech. Microeng. **12**, 702 (2002).
6. G. N. Nielson, D. Seneviratne, F. Lopez-Royo, P. T. Rakich, H. L. Tuller, and G. Barbastathis, IEEE Photon. Technol. Lett. **17**, 1190 (2005).
7. G. N. Nielson, "Micro-opto-mechanical switching and tuning for integrated optical systems," Ph.D. thesis (MIT Archives, 2004).
8. D. Sarid, *Scanning Force Microscopy with Applications to Electric, Magnetic, and Atomic Forces* (Oxford U. Press, 1994).
9. R. S. Tucker, D. Baney, W. Sorin, and C. Flory, IEEE J. Sel. Top. Quantum Electron. **8**, 88 (2002).